Progress in Nuclear Energy, Vol. 27, No. 4, pp. 255–295, 1992.
Printed in Great Britain.

0149–1970/92 $15.00

A VOID FRACTION CORRELATION FOR GENERALIZED APPLICATIONS

B. CHEXAL,* G. LELLOUCHE,† J. HOROWITZ‡ and J. HEALZER

*Electric Power Research Institute, Palo Alto, CA 94303, U.S.A.
†Technical Data Services, Chicago, IL 60660, U.S.A.
DuPage Computer Applications, Inc., Woodridge, IL 60517, U.S.A.
S. Levy Incorporated, Campbell, CA 95008, U.S.A.

Abstract - A void fraction correlation has been developed to cover the full range of pressures, flows, void fractions, and fluid types (steam-water, air-water, hydrocarbons, and oxygen). The correlation, referred to here as the Chexal-Lellouche correlation, has been qualified against several sets of steady-state two-phase/two-component flow test data that cover a wide range of thermodynamic conditions and geometries typical of PWR and BWR fuel assemblies as well as for pipes up to 450 mm in diameter. The correlation is based on a drift flux model and determines the drift flux parameters, C_o and V_{gj} both cocurrent and countercurrent two-phase flows for the full range of pressures, flows and void fractions. The correlation is available as a source code module for inclusion into any thermal-hydraulic computer program, and as an interactive personal computer program. The correlation is continuous and does not depend on flow regime maps or spline fitting.

1. INTRODUCTION

The ability to predict accurately the thermal hydraulic behavior of light water reactors during normal operation or during an accident requires correct simulation of steam and water flows in the primary and secondary coolant systems. Since in two-phase flows there is always some relative motion of one phase with respect to the other, such flow problems should be formulated in terms of two velocity fields. A general transient two-phase flow problem can be formulated by using a two-fluid model (Ishii, 1975) or a drift flux model (Zuber and Findlay, 1965 and Zuber, 1967).

In the two-fluid model, each phase is considered separately, hence the flow model is formulated in terms of two sets of conservation equations governing the balance of mass, momentum, and energy of each phase. However, the introduction of two momentum equations in a two-fluid model presents considerable difficulties because of mathematical complications and of uncertainties in specifying interaction terms, e.g., the interfacial drag, between the two phases. Phasic interaction models typically depend on the flow regime which, in general, varies with mass flow rate and the void fraction. Changes in the flow regime during a flow transient introduce added complications in the calculation of two-phase flow parameters. Numerical instabilities caused by improper choice of interaction terms in the phasic momentum equations are quite common, and therefore very careful studies on the phase interaction equations are required in the two-fluid model formulation.

This paper describes an empirical drift flux correlation that eliminates the need to know the flow regime before void fraction predictions can be made. When applied to steam-water systems, the correlation covers a wide range of pressures, flows and void fractions for

cocurrent or countercurrent vertical flow conditions. The advantages of the drift flux formulation, in addition to its simplicity, are that it provides a means for accounting for both the relative velocity between the phases and for non-uniform flow and density distributions. These are accounted for separately in the drift flux formulation with correlation parameters.

The data base for which comparisons to the present correlation have been made include the following types of data:

Steam-water

For steam-water flows, the correlation has been qualified against a variety of data at conditions typical of light water reactors operating at accident conditions. These include:

- High pressure - high flows
- High pressure - low flows
- Low pressure - low flows
- Horizontal flows
- Countercurrent flooding limitation (CCFL)
- Cocurrent down flows

Air-water

For air-water systems, the correlation has been qualified against cocurrent flow data over a wide range of diameters and flow orientations. Comparisons to air-water CCFL data have also been made.

Refrigerants

To illustrate its use for other two-phase systems, the correlation has been used to predict cocurrent upflow, horizontal flow and downflow data taken with several different refrigerants. This comparison is found in Chexal, et al., 1991.

Table 1-1 summarizes the void fraction data used for qualification of the correlation. The range of parameters shown in the table for steam-water data would appear to cover all flow regimes with the possible exception of fully developed annular dispersed flow, below pressures of about 35 bars.

2. DRIFT FLUX PARAMETER CHARACTERISTICS

A brief historical perspective on the drift flux model is presented in Appendix A. The general drift flux formulation for void fraction is given by:

$$\langle\alpha\rangle = \frac{\langle j_g \rangle}{C_o \langle j \rangle + \bar{V}_{gj}}$$

where $\langle j \rangle$ and $\langle j_g \rangle$ are the mixture and vapor volumetric flux, $\bar{V}_{gj}$ drift velocity and C_o the distribution parameters.

Some drift flux correlations provide a better fit to void fraction data than others. The reasons for such behavior are in the characteristics of the drift flux parameters C_o and $\bar{V}_{gj}$. Of particular interest are the limiting or end point values of these parameters and what ever additional requirements that can be justified. For physical systems of interest, phase

Table 1-1. Chexal-Lellouche Void Fraction Correlation Steam Water Data

DIABATIC DATA

PARAMETER	RANGE
Number of Data	1427
Void Fraction	0.01 - 0.95
Mass Flux	0.01 - 2100 kg/s-m^2
Pressure	1 - 145 bars
Heat Flux	1.3 - 1130 kw/m^2
Subcooling	0 - 30°C
Geometry	bundle and tube ($0.009 \leq D_H \leq 0.048$ m)

ADIABATIC DATA

PARAMETER	RANGE
Number of Data	521
Void Fraction	0.05 - 0.98
Mass Flux	0.01 - 2550 kg/s-m^2
Pressure	1 - 180 bars
Geometry	tube ($0.005 \leq D \leq 0.456$ m)

AIR-WATER DATA

PARAMETER	RANGE
Number of Data	1401
Void Fraction	0.01 - 0.98
Mass Flux	0.04 - 5500 kg/s-m^2
Pressure	1 - 6.8 bars
Geometry	tube and channel ($0.01 \leq D \leq 0.3$ m)

REFRIGERANT DATA

PARAMETER	RANGE
Type of Refrigerants	R11,R12,R22,R113,R114, Oxygen
Number of Data	4356
Void Fraction	0.01 - 0.99
Mass Flux	70 - 4100 kg/s-m^2
Pressure	1 - 23 bars
Geometry	tube ($0.03 \leq D \leq 0.12$ m)

velocities and void fractions should be continuous except at two-phase/single-phase interfaces and/or at geometric discontinuities. Thus, the functional form of C_o and $\bar{V}_{gj}$ should be continuous, have finite first derivatives and should restrict the void fraction to be in the range from zero to one. Also, the behavior of C_o and $\bar{V}_{gj}$ are of interest both as the void fraction approaches zero and one and as the pressure approaches the critical pressure. The success of the Chexal-Lellouche correlation in fitting a wide range of data has been at least in part due to efforts to insure the drift flux parameters obey these rules.

Critical pressure limit

When the pressure is at and above the critical pressure ($p \geq p_{CR}$), the phases cannot be distinguished; therefore, flow must be homogeneous and $\bar{V}_f = \bar{V}_g$. This condition implies that for all void fractions:

$$\lim_{p \to p_{CR}} \bar{V}_{gj} = 0$$

$$\lim_{p \to p_{CR}} C_o = 1$$

These requirements follow from the desire for homogeneous flow after averaging of the parameters.

Zero pressure limit

As the pressure goes to zero, $1/\rho_g$ becomes infinite. Therefore, any voidage that is formed leads to the void fraction going to one (and $\bar{V}_g$ becoming infinite). In this situation, the expression for vapor velocity (see Eq. A-19) as $\rho_g/\rho_f \to 0$ must reduce to

$$\lim_{\substack{\alpha \to 1 \\ p \to 0}} \bar{V}_g = \left[\frac{\dfrac{C_o G_o}{\rho_f} + \bar{V}_{gj}}{1 - C_o} \right] = \infty$$

which leads to $C_o = 1$.

Limit as void fraction goes to one

As the void fraction goes to one, the distribution parameter and drift velocity (see Eqs. A-9 and A-11) must have the following behavior:

$$\lim_{\alpha \to 1} C_o = 1$$

$$\lim_{\alpha \to 1} \bar{V}_{gj} = 0$$

As the flow becomes all vapor it must again behave as a homogeneous mixture.

Zero void fraction limit

Although all the above limits are either directly based on analysis or physics, the limits as the void fraction goes to zero are not as easily determined. It is possible to show different limits for C_o and $\bar{V}_{gj}$ as the void fraction goes to zero depending on how it approaches zero. Because of this situation, the following limits are used:

$$\lim_{\alpha \to 0} \bar{V}_{gj} > 0$$

$$\lim_{\alpha \to 0} C_o = 0$$

The implication is that $\bar{V}_g$ will generally be greater than $\bar{V}_f$ when voidage starts, which is reasonable for voids formed in the thermal boundary sublayer where the local liquid velocity approaches zero and leads to

$$\lim_{\alpha \to 0} \bar{V}_g = \bar{V}_{gj}(0)$$

Thus, voids are formed with a specific velocity. Although it would seem that distributed voids should go to the liquid velocity as the void fraction approaches zero, the condition given above appears reasonable for void fractions as low as 2% as will be seen in the section on data comparisons.

Boundedness and continuity

Physically, the void fraction must lie between zero and one, independently of the values of C_o and $\bar{V}_{gj}$, whether in cocurrent or countercurrent flow. This requirement means that the calculated void fraction should be between zero and one. C_o or $\bar{V}_{gj}$ may be double-valued if any of the first derivatives are infinite at some value in parameter space. As a result, the void fraction will be double valued at that point. This situation will lead to the divergence of space and time derivatives of the void fraction at that point even if the velocities are continuous (i.e., both α and $\bar{V}_g$ jump while $\alpha\bar{V}_g$ is continuous). Such discontinuities can propagate in space-time similarly to a shock front. Discontinuities of this sort behave exactly the same as a shock except that the velocity of propagation is the local velocity, not the sonic velocity. It is for this reason that the use of flow regime maps, even with some smoothing, can lead to numerical oscillations. Even finite jumps in the derivatives ($d\bar{V}_{gj}/d\alpha$ or $dC_o/d\alpha$) can lead to distortions in the solutions for the void fraction.

None of this denies that jumps in void fraction and velocity take place at a true discontinuity, such as a sharp geometry change in the flow path, or at an interface between the two-phase mixture and a vapor. However, these are the only places where such discontinuous behavior is real.

To summarize the limiting behavior of the drift flux parameters:

1. High pressure behavior

$$\lim_{p \to p_{CR}} \bar{V}_{gj} = 0$$

$$\lim_{p \to p_{CR}} C_o = 1$$

2. Low pressure, high void fraction behavior

$$\lim_{\substack{\alpha \to 1 \\ p \to 0}} C_o = 1$$

$$\lim_{\substack{\alpha \to 1 \\ p \to 0}} \frac{d(1/C_o)}{d\alpha} = 1$$

3. High void fraction behavior

$$\lim_{\alpha \to 1} C_o = 1$$

$$\lim_{\alpha \to 1} \bar{V}_{gj} = 0$$

4. Initiation of voidage

$$\lim_{\alpha \to 0} C_o = 0$$

5. Smoothness

$\bar{V}_{gj}$ and C_o are continuous with small or no discontinuities in their first derivatives and predicted void fractions lie between zero and one.

3. THE CHEXAL-LELLOUCHE VOID FRACTION CORRELATION

Development of the present correlation

The Chexal-Lellouche void fraction correlation is flow regime independent and employs the functional dependencies of the drift flux parameters just discussed. The salient features of this correlation are that

- it is continuous with pressure and flow direction;
- it covers a large range of sizes, pressures, and flows;
- it eliminates the need for a flow regime map;
- it reproduces the measured void fraction for a wide variety of data for two-phase/two component mixtures; and
- it can also predict the CCFL line.

The correlation was originally developed to fit upflow steam-water void fraction measurements over a wide range of experimental conditions (Lellouche and Zolotar, 1982, Lellouche, 1988, and Chexal and Lellouche, 1986). The correlation has recently been revised to better predict downflow data, horizontal flow data, air-water data and refrigerant data. The major elements of the correlation revision have been to modify the drift flux parameter to account for flow orientation and to revise the distribution parameter correlation to provide a better fit to void fraction data for other fluids. The correlation form for vertical upflow steam-water data remains the same over the parameter range of the earlier correlation (Chexal et al., 1986).

The ability to predict data over a wide range of conditions has been an important feature that has distinguished the present correlation over others. In a recent study (Chexal et al., 1991) the correlation was compared with seven other correlations to void data over a wide range of conditions. The present correlation was shown to be more successful than others in predicting the data. This feature has also made the correlation useful in computer programs used for thermal-hydraulic analysis. Since the correlation is continuous, it is well suited for computer application, particularly if a wide range of thermodynamic conditions are to be simulated. The correlation is available as options in several computer codes including RETRAN03 (McFadden et al., 1991). Experience in using the correlation has indicated that for some transients where there is a large change in system pressure or flow, the use of the Chexal-Lellouche correlation can greatly reduce computational time required (Peterson, 1991).

The correlation has been used as a benchmark for the void calculation by the TRAC code (Cappiello, 1991).

Correlation parameters

As noted earlier, the general drift flux model formulation for void fraction is given by:

$$\langle\alpha\rangle = \frac{\langle j_g \rangle}{C_o\,(\langle j_g \rangle + \langle j_g \rangle) + \bar{V}_{gj}} \tag{3-1}$$

where

$\langle j_f \rangle$, $\langle j_g \rangle$ = the liquid and vapor volumetric flux

C_o = the distribution parameter

$\bar{V}_{gj}$ = the drift velocity parameter

Separate correlations have been developed for the distribution parameter and the drift velocity. As discussed earlier, attention is given to the form of these correlations to insure they are continuous and behave properly at the correlation limits.

Distribution parameter

The distribution parameter, C_o, for a two-phase mixture flowing at any angle, where the angle is measured from the vertical axis, is the weighted average of values for horizontal and vertical flow.

$$C_o = F_r C_{ov} + (1-F_r)\, C_{oh} \tag{3-2}$$

where C_{ov} and C_{oh} are the distribution parameters evaluated for vertical and horizontal flow and F_r is a flow orientation parameter defined as

for $Re_g \geq 0$

$$F_r = (90°-\theta)/90° \text{ for } (0° \leq \theta \leq 90°) \tag{3-3a}$$

for $Re_g < 0$

$$F_r = \begin{cases} 1 \text{ for } (\theta < 80°) \\ (90°-\theta)/10° \text{ for } (80° < \theta < 90°) \end{cases} \tag{3-3b}$$

where

θ = pipe orientation angle measured from the vertical axis

Re_g = local vapor superficial Reynolds number

= $W_g D_H / \mu_g A$

W_g = vapor flow

D_H = hydraulic diameter

A = total flow area

μ_g = vapor viscosity

The flow orientation parameter is illustrated in Fig. 3-1 for four different cases, including vertical up and downflow, horizontal flow and inclined flow. Note that in all cases, the pipe orientation angle, θ, is in degrees measured from vertical. As shown, θ=0° is for a vertical pipe and θ=90° is for a horizontal pipe. The angle is always in the limits of ($0° \leq \theta \leq 90°$).

Vertical flow

For vertical pipe (θ=0°), the volumetric fluxes, j_f and j_g, are taken as positive if both phases are flowing upward and negative if both phases are flowing downward. For countercurrent flow, the vapor velocity is always positive (upward) and the liquid velocity is always negative (downward). Countercurrent flow is only considered for vertical flows. The distribution parameter for vertical flow is given by:

for $Re_g \geq 0$

$$C_{ov} = L/[K_o + (1-K_o) <\alpha>^r] \tag{3-4a}$$

for $Re_g < 0$

$$C_{ov} = \max \begin{cases} L/[K_o + (1-K_o) <\alpha>^r] \\ V_{gj}^o (1-<\alpha>)^{0.2}/(|<j_f>| + |<j_g>|) \end{cases} \tag{3-4b}$$

where

V_{gj}^o = defined later by Eq. 3-24

L = Chexal-Lellouche fluid parameter

The choice of the L parameter is important in the fitting of the correlation to the void fraction data. The parameter has been defined to insure continuous behavior of the distribution parameter and therefore proper behavior at the void fraction in the limit between zero and one. Different forms of L are used with different fluids. For steam-water mixtures the form of L is selected to insure proper behavior as the pressure approaches the critical pressure,

$$L = \frac{1 - \exp(-C_1 <\alpha>)}{1 - \exp(-C_1)} \tag{3-5}$$

where,

$$C_1 = 4 p_{crit}^2/[p (p_{crit}-p)] \tag{3-6}$$

For, air-water mixtures, the pressure range of available data is not large and a form of L was used that is only dependent on the void fraction and flow orientation,

$Re_g \geq 0$

$$L = \min [1.15<\alpha>^{0.45}, 1.0] \tag{3-7}$$

$Re_g < 0$

$$L = \min [1.05<\alpha>^{0.25}, 1.0] \tag{3-8}$$

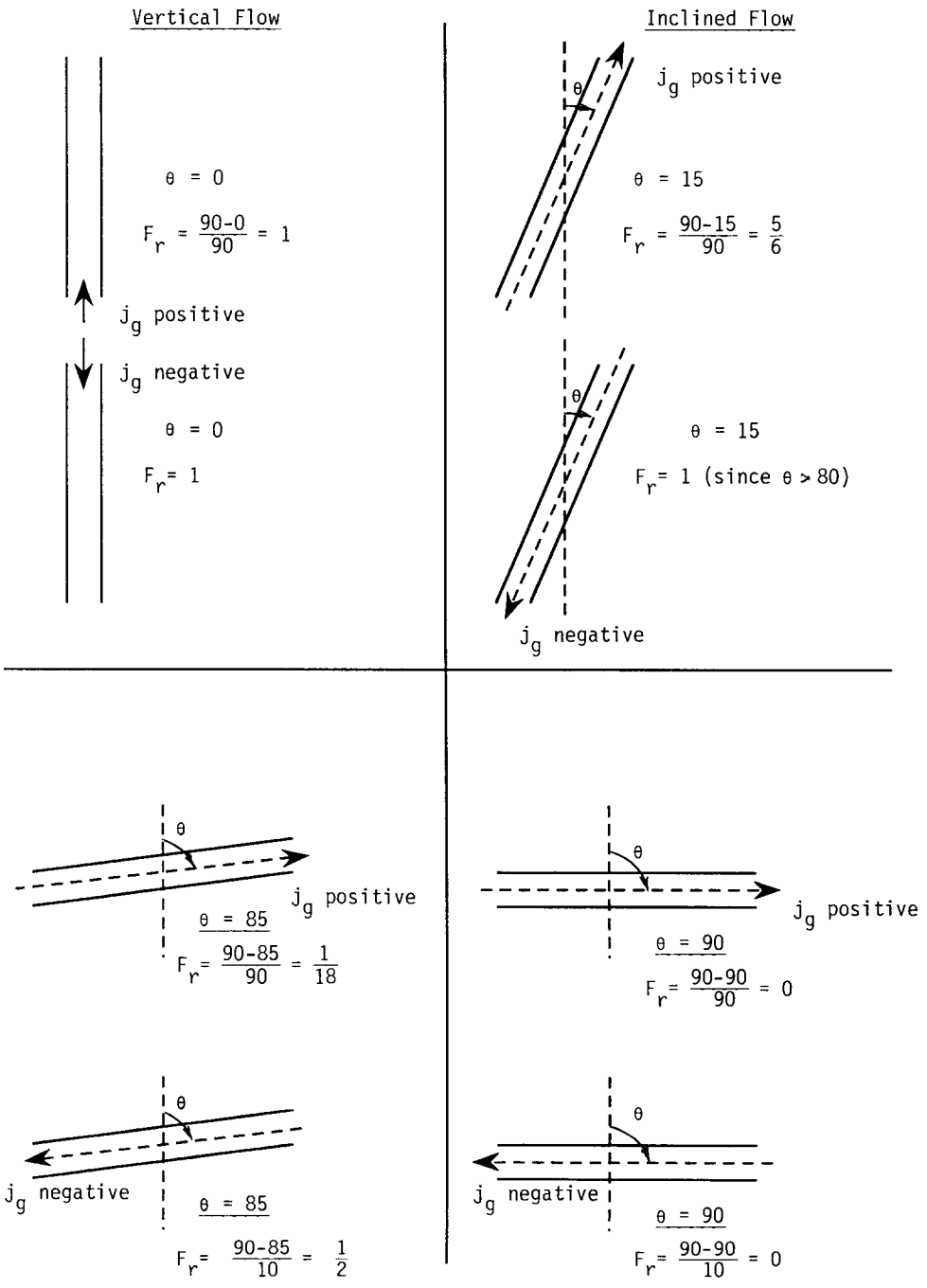

Fig. 3-1. Flow Orientation Parameter

For refrigerants as well, the pressure range in the available data is not large and L is correlated in terms of the void fraction and flow orientation,

$Re_g \geq 0$

$$L = \alpha^{0.025\ (1+10<\alpha>)}\ \exp[0.5(1-<\alpha>)] \tag{3-9}$$

$Re_g < 0$

$$L = [1 - \exp(-100<\alpha>)][.02(<\alpha>+4) - .074\ <\alpha>^2(1-<\alpha>)] \tag{3-10}$$

Other variables in the distribution parameter correlation are defined as,

$$K_o = B_1 + (1-B_1)\ (\rho_g/\rho_f)^{1/4} \tag{3-11}$$

$$r = (1.0 + 1.57\ \rho_g/\rho_f)/\ (1-B_1) \tag{3-12}$$

$$B_1 = \min\ (0.8,\ A_1) \tag{3-13}$$

$$A_1 = 1/[1 + \exp\ (-Re/60{,}000)] \tag{3-14}$$

$$Re = \begin{cases} Re_g \text{ if } Re_g > Re_f \text{ or } Re_g < 0.0 \\ Re_f \text{ if } Re_g \leq Re_f \end{cases} \tag{3-15}$$

$$Re_f = \text{local liquid Reynolds number} = \frac{W_f\ D_H}{\mu_f A} \tag{3-16}$$

$$Re_g = \text{local vapor Reynolds number} = \frac{W_g\ D_H}{\mu_g A} \tag{3-17}$$

The sign convention for all Reynolds numbers, Re, Re_f and Re_g is the same as the sign convention for the individual flows.

Horizontal flow

For horizontal flow (θ=90°), the void fraction correlation considers only cocurrent flows. Horizontal countercurrent flow has not yet been included in the data base. The volumetric fluxes for horizontal flow are always taken as positive; negative volumetric fluxes should not be used. The distribution parameter for horizontal flow is given by

$$C_{oh} = [1 + <\alpha>^{0.05}\ (1-<\alpha>)^2]\ C_{ov} \tag{3-18}$$

where C_{ov} is defined by Eq. 3-4a above, and evaluated for positive vapor Reynolds numbers. For horizontal flows, the Chexal-Lellouche fluid parameter used in C_{ov} is defined as follows:

steam-water, (the same as described earlier, Eq. 3-5)

$$L = \frac{1 - \exp(-C_1\langle\alpha\rangle)}{1 - \exp(-C_1)}$$

air-water,

$$L = \min\ [1.125\langle\alpha\rangle^{0.6},\ 1.0] \tag{3-19}$$

refrigerants,

$$L = \langle\alpha\rangle[1.375 - 1.5(\langle\alpha\rangle-0.5)^2] \tag{3-20}$$

All other parameters are defined as for vertical flows, with positive volumetric fluxes.

As noted earlier for both vertical and horizontal steam-water flows, the Chexal-Lellouche fluid parameter is a function of both pressure and void fraction while the parameter is only a function of void fraction for air-water and refrigerant flows. Since much of the air-water data is at low pressure, there is no basis for introducing a pressure variation. Figs. 3-2 and 3-3 show the Chexal-Lellouche fluid parameter variation with void fraction. For most cases the parameter is near 1.0 at void fraction greater than 0.6. With appropriate adjustment to this parameter, the general form of the void correlation should be applicable to any fluid.

Drift velocity

The drift velocity, $\bar{V}_{gj}$ for cocurrent upflow and pipe orientation angles ($0°<\theta<90°$) is defined as

$$\bar{V}_{gj} = Fr\ V_{gjv} + (1-Fr)\ V_{gjh} \tag{3-21}$$

where V_{gjv} and V_{gjh} are the drift velocities for vertical and horizontal flow and F_r is the flow orientation parameter defined by Eqs. 3-3a and 3-3b. For cocurrent downflow, the drift velocity is defined as

$$\bar{V}_{gj} = Fr\ V_{gjv} + (Fr-1)\ V_{gjh} \tag{3-22}$$

Vertical flow

Like the distribution parameter, the drift velocity for a vertical pipe ($\theta=0°$), V_{gjv}, covers cocurrent upflow and downflow and countercurrent flow. The drift velocity for vertical flow is given by

$$V_{gjv} = V_{gj}^{o}\ C_9 \tag{3-23}$$

where

$$V_{gj}^{o} = 1.41 \left[\frac{(\rho_f-\rho_g)\sigma\ g g_c}{\rho_f^2} \right]^{0.25} C_2\ C_3\ C_4 \tag{3-24}$$

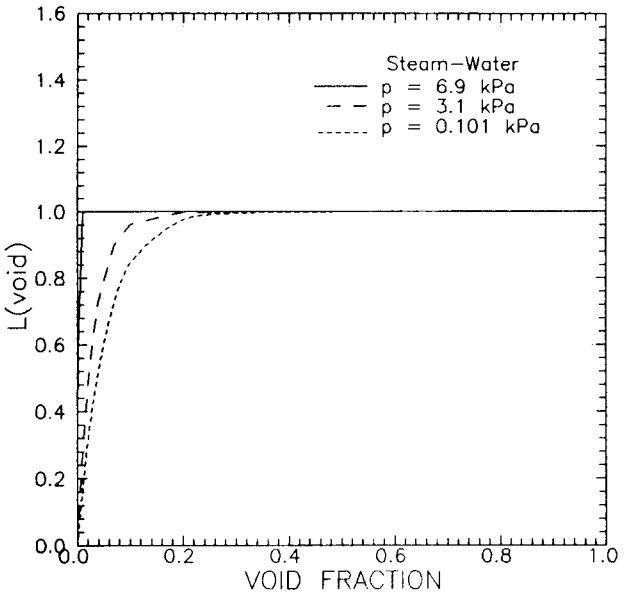

Fig. 3-2. Chexal-Lellouche Fluid Parameter for Steam-Water

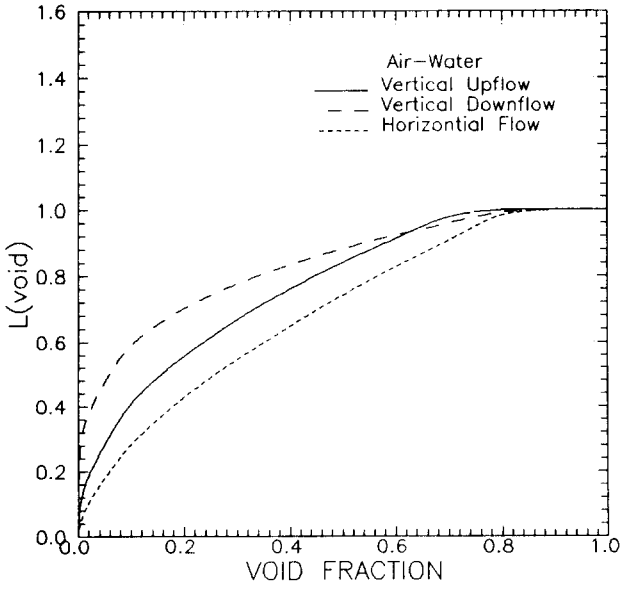

Fig. 3-3. Chexal-Lellouche Fluid Parameter for Air-Water

for $Re_g \geq 0$

$$C_9 = (1-\langle\alpha\rangle)^{B_1} \tag{3-25}$$

for $Re_g < 0$

$$C_9 = \min \begin{cases} 0.7 \\ (1-\langle\alpha\rangle)^{0.65} \end{cases} \tag{3-26}$$

Other parameters are defined as

for $(\rho_f/\rho_g) \leq 18$

$$C_2 = 0.4757\ [\ln\ (\rho_f/\rho_g)]^{0.7} \tag{3-27}$$

for $(\rho_f/\rho_g) > 18$

$$C_2 = \begin{cases} 1 \text{ if } C_5 \geq 1 \\ 1/\{1-\exp\ [-C_5/(1-C_5)]\} \text{ if } C_5 < 1 \end{cases} \tag{3-28}$$

where

$$C_5 = \sqrt{150/(\rho_f/\rho_g)} \tag{3-29}$$

$$C_4 = \begin{cases} 1 \text{ if } C_7 \geq 1 \\ 1/[1-\exp\ (-C_8)] \text{ if } C_7 < 1 \end{cases} \tag{3-30}$$

$$C_7 = (D_2/D_H)^{0.6} \tag{3-31}$$

$$C_8 = \frac{C_7}{1 - C_7} \tag{3-32}$$

$$D_2 = \text{Normalizing diameter, 0.09144 m} \tag{3-33}$$

The parameter, C_3, is determined based on the direction of the gas and liquid flows. It is continuous as the two directional boundaries are crossed. The values of C_3 for the three types of flows (cocurrent upflow, cocurrent downflow, and countercurrent flow) are given by

Upflow (both $\langle j_f \rangle$ and $\langle j_g \rangle$ are positive)

$$C_3 = \max \begin{cases} 0.50 \\ 2\ \exp\ [-\ |Re_f|/60{,}000] \end{cases} \tag{3-34}$$

Downflow (both $\langle j_f \rangle$ and $\langle j_g \rangle$ are negative)

$$C_3 = 2\,(C_{10}/2)^{B_2} \tag{3-35}$$

$$C_{10} = 2 \exp\{(|Re_f|/350{,}000)^{0.4} - 1.75\,(|Re_f|)^{0.03} \exp\left\{\frac{-|Re_f|}{50{,}000} \cdot \left(\frac{D_1}{D_h}\right)^2\right\} + \left(\frac{D_1}{D_h}\right)^{0.25} \cdot |Re_f|^{0.001} \tag{3-36}$$

$$B_2 = [1/(1 + 0.05(|Re_f|/350{,}000)]^{0.4} \tag{3-37}$$

$$D_1 = \text{Normalizing diameter} = 0.0381 \text{ m} \tag{3-38}$$

Countercurrent Flow ($\langle j_g \rangle$ is positive and $\langle j_f \rangle$ is negative).

For clarity, this procedure is described in two parts - one relating to prediction of the countercurrent flooding limit (CCFL) and the other relating to below the CCFL line, i.e., countercurrent flow.

On the CCFL line

$$C_3 = 2\,(C_{10}/2)^{B_2} \tag{3-39}$$

In the region of countercurrent flow, there are two solutions for void fraction ($\langle \alpha_1 \rangle$ and $\langle \alpha_2 \rangle$) at every point. The desired void fraction, $\langle \alpha_{des} \rangle$, known a priori from pressure drop or other information must be used in selecting the appropriate C_3 as follows:

for $\langle \alpha_{des} \rangle = \max(\langle \alpha_1 \rangle, \langle \alpha_2 \rangle)$

$$C_3 = 2(C_{10}/2)^{B_2} \tag{3-40}$$

for $\langle \alpha_{des} \rangle = \min(\langle \alpha_1 \rangle, \langle \alpha_2 \rangle)$

$$C_3 = \min \begin{cases} 2(C_{10}/2)^{B_2} \left(\dfrac{\langle j_f \rangle}{\langle j_f^* \rangle}\right) + 2\left(1 + \dfrac{|Re_f|}{60{,}000}\right)\left(1 - \dfrac{\langle j_f \rangle}{\langle j_f^* \rangle}\right) \\ 2(C_{10}/2)^{B_2} \end{cases} \tag{3-41}$$

Where $\langle j_f^* \rangle$ is the value on the CCFL line corresponding to $\langle j_g \rangle$ and is calculated using C_3 as defined by Eq. 3-39.

Horizontal flow

When a drift-flux model is applied to horizontal flow, the drift velocity, $\bar{V}_{gj}$ is often set to zero. This would certainly seem to be reasonable if $\bar{V}_{gj}$ were considered to be buoyancy related. Yet from its definition (see Eq. 2-9), there is no reason to believe that it should

go to zero in horizontal flow. Indeed when the horizontal flow data is analyzed (actually for steam/water and air/water) it becomes clear that $\bar{V}_{gj} \neq 0$ is necessary if any reasonable fit is to be made. For horizontal flow the void fraction correlation considers only cocurrent flows. The drift velocity for horizontal flow, V_{gjh}, is evaluated with Eq. 3-23, using positive values of the volumetric fluxes.

Units

The correlation is the same in either British or SI units, as long as consistent units are used throughout. C_0 has no units and $\bar{V}_{gj}$ has the units of a velocity and should be consistent with the units used for the volumetric fluxes.

Subcooled boiling model

Data comparisons in Section 4 include some diabatic data. For these comparisons, a subcooled boiling model is needed. For the data comparisons shown, a mechanistic subcooled boiling model by Lellouche (1988) has been used. This model, which is described in more detail in Appendix B, expresses the derivative of the flow quality in terms of the derivative of the equilibrium quality and other parameters of the heated channel flow:

$$\frac{dX}{dz} = \frac{S(dX_e/dz) - C(X-X_e)/(1-X)}{1 + \frac{\rho_l}{\rho_g}(X-X_e)/(1-X)} \tag{3-42}$$

where

X = channel flow quality = W_g/W

z = distance along the channel

ρ_l, ρ_g = the subcooled liquid and saturated vapor densities

S = $(h_B + h_{fc}/2)/(h_B + h_{fc})$

C = $4(h_c + Sh_{fc})/(W\ D_H\ C_{pl}/A)$

h_c, h_{fc}, h_B = condensation, forced convection and boiling heat transfer coefficients

W_g = channel flow rate of vapor

W = channel flow rate

C_{pl} = liquid specific heat

X_e = channel equilibrium quality = $(h-h_f)/h_{fg}$

h = two-phase (i.e. mixture) enthalpy

h_f, h_{fg} = saturated liquid enthalpy and heat of vaporization

This equation is solved numerically for the flow quality along the channel, which is then used to calculate the void fraction.

4.0 COMPARISON WITH STEAM-WATER DATA

Qualification of the Chexal-Lellouche correlation has concentrated on steam-water data since it is anticipated that this will be the most important application of the correlation. Sources for steam-water data are discussed in this section.

Data sources

Although large amounts of void fraction data have been taken, a relatively small fraction of that data and in particular the steam-water data, is in the public domain. A still smaller fraction of the steam-water data are for geometries of interest. The data base for the present correlation is a mix of public and proprietary data. Part of the data has been used to establish the drift flux model and the rest of the data has been used for validation of the Chexal-Lellouche correlation.

This data base consists of two basic geometries:

1. Tubes (some under one inch to over two feet in diameter);
2. Assemblies (up to full size BWR fuel bundles).

The data covers cocurrent upflow and downflow and flow at CCFL conditions. It has not been possible to locate countercurrent flow data, off the CCFL line, hence the modeling of this region is not yet verifiable.

Void measurements

The experimental techniques used to determine void fraction were:

1. Gamma Spectroscopy;
2. Quick closing valves;
3. Pressure drops between experimental stations.

None of these methods measure void fraction. The first measures a change in gamma flux (or intensity) which, through calibration, leads to an estimate of global density. The third measures the sum of head and friction losses, and changes in momentum flux between the two stations. This sum, coupled with a model for friction and momentum flux changes, leads to an estimate of the average density between the experimental stations. These methods measure one aspect or another of density, and only the second method provides a direct estimate of the density. The other methods require modeling or extensive secondary calibration. The primary reduction of the experimental data is to density (ρ_{exp}).

Interpreting void fraction from density

In any two-phase (gas-liquid) mixture, the density is related to the void fraction through the simple equation:

$$\rho_{exp} = \rho_{\ell}(1-\alpha) + \alpha\rho_g$$

The phasic densities, ρ_{ℓ}, and ρ_g depends on the experiment. If, for example, a single beam γ-densitometer measuring along a diameter of a tube is used, the ρ_{exp} is actually a diametral density. The methods used by the experimenter to pass from the measurement to the void fractions are not always simple and often it would be easier if the experimenter also reported the densities as well as the void fraction, but, in any event, the above sets of experimental data have been accepted as the data base.

Data validation

Three rules were used to accept or reject a data set:

1. Scatter in the α, z plane;

2. Scatter in the α, X_f plane;

3. Reported errors.

The (α, z) plane is the plane up or along the experimental section. The void fractions can be shown to be a monotonically non-decreasing function along the flow path as long as the flow path is not actively cooled. Therefore, if the experimental void fractions jump around with $d\alpha/dz < 0$ especially in a heated section, then the experiment is considered to be less reliable.

The use of the α, X_f plane is a consequence of the relationship between void fraction and the flowing quality; thus:

$$\alpha = \frac{X_f}{X_f + R\,S(1-X_f)}$$

$$R = \rho_g/\rho_\ell \text{ (density ratio)}$$

$$S = \bar{V}_g/\bar{V}_\ell \text{ (slip ratio)}$$

S is usually a weak function of hydraulic diameter, a weak function of pressure, a weak function of total flow rate, and a strong function of the void fraction. Thus, at a given pressure that defines R, the equation is nearly uniquely defined by X_f. That is, independently of how a value of X_f was determined, α will always have the same value with only weak variations caused by diameter and flow rate. Thus, if X_f is calculated for the experiment the experimental α, X_f should fit a smooth line. If the scatter is large, a degree of unreliability can be ascribed to the data.

Reported errors indicate the experimenters belief in his own data. As the boiling process is inherently statistical, most measurements are variable to a degree even at "steady state." Data accepted here have reported ± 5% variation in the actual void fraction ($\alpha \pm \Delta\alpha$ with $\Delta\alpha = 0.05$).

These three criteria have been factored in and the data sets listed are accepted as sufficiently reliable.

Data base details

Rather than consider the experimental steam-water data base one set at a time, they are discussed below in several distinct groups, each of which provides a different aspect of the pressure, flow, and geometry parameter plane.

The statistics used for data comparisons are defined as follows:

error: $$\varepsilon_i = \langle\alpha_{i,meas}\rangle - \langle\alpha_{i,calc}\rangle$$

mean error: $$\hat{\varepsilon} = \frac{1}{N}\sum_{i=1}^{N}\varepsilon_i$$

$$\text{standard deviation:} \quad s = \left[\frac{1}{N-1} \sum_{i=1}^{N} (\varepsilon_i - \hat{\varepsilon})^2 \right]^{1/2}$$

Data comparisons

It is important to note that the Chexal-Lellouche correlation is not the result of regression analysis nor have all data sets or any subsets been grouped for determining sample mean and variance.

In order to review the data as a composite (even though it is not assumed that the data sets can be combined statistically) the data has been shown in plots which compare predicted versus measured values for vertical upflow, horizontal flow, cocurrent down flow and CCFL. The data base of cocurrent steam-water data is listed in Table 4-1 and the countercurrent limit data to which the correlation has been compared is listed in Table 4-2.

Vertical upflow data

The data base of vertical upflow steam-water data includes both diabatic and adiabatic data. Rod bundle and heated tube data from a variety of sources and over a wide range of pressures and flow conditions have been used for correlation qualification.

High pressure-high flow data

These are conditions typical of a BWR at normal operation and of steam generators in a PWR at normal operation. The ability to model these conditions correctly helps provide an understanding of system responses for manual operational conditions and transients.

Nyland (1967 through 1970) - This is 6 and 36 rod bundle diabatic data at protypical light water reactor conditions.

Kasai et al. (1985) - This is adiabatic data in a 4.6 mm diameter tube over a range of mass flows.

Bartolomei (1982) - This data in a 12 mm diameter tube covers a wide range of pressures and flows.

High pressure-low flow data

These conditions are typical of a small break LOCA. During such transients, it is important to predict the extent of uncovering of the fuel, which is dependent on both the liquid inventory and the core void fraction distributions. These conditions may also occur during BWR Anticipated Transient Without Scram (ATWS) if the downcomer water level is lowered to the top of the active fuel to reduce power.

Anklam (1982) - This is 64-rod heated bundle data with dimensions typical of a 17x17 PWR bundle.

Seedy-Muralidhoran (1982) - This data taken in the TLTA facility were a source of low-flow boil off tests.

Low pressure-high flow data

Turnage-Davis (1979) - This data is a 89 mm tube covers a range of mass flows.

Table 4-1. Diabatic steam-water void fraction data

Experiment [ref]	Test Geometry	Hyd Dia mm (ft)	Length m (ft)	Pressure bar (psia)	Mass Flow kg/s-m2 (Mlb/hr-ft2)	Heat Flux kW/m2 (MBtu/hr-ft2)	Number Data Pts	Mean Error	Standard Deviation
Nylund* [1967 through 1970]	6 & 36 rod bundle	13.4, 36.5, 47.7 (.044, .12, .15)	4.3, 3.7 (14.5, 12)	40 - 62 (585 - 900)	1100 - 1360 (0.8 - 1.1)	380 - 600 (.12 - .19)	765	-.003	.032
Seedy-Muralidhoran* [1982]	64 rod bundle	13.4 (.044)	3.8 (12.5)	13.4 - 54.5 (195 - 790)	11 - 14 (.008 - .013)	28, 44 (.009, .014)	37	.043	.037
Anklam* [1982]	64 rod bundle boiloff	10.7 (.035)	3.7 (12)	75.8, 41.2 (1100, 600)	5 - 34 (.004 - .025)	10 - 76 (.003 - .024)	53	-.011	.074
Hall-Ardron [1978]	19 rod bundle boiloff	33 (.108)	0.46 (1.5)	1 -4 (14.5 - 58)	.01 - .66 (.00001-.00049)	1.3 -41.3 (.0004 - .0131)	18	-.045	.032
Wong-Hochreiter* [1981]	117 rod bundle	11 (.036)	3.7 (12)	1.4 - 4.1 (20 - 60)	11 (.008)	31 - 32.5 (.0098 - .0103)	14	.007	.071
Jowitt* [1982]	61 rod bundle boiloff	9.1 (.03)	3.6 (11.8)	2 - 40 (29 - 580)	.4 - 10 (.0003 - .0077)	1.3 - 18.3 (.0004 - .0058)	117	-.004	.063
Bartolomei [1982]	tube	12 (.04)	0.8-1.5 (2.6-5.0)	30-145 (440-2100)	500-2100 (0.4-1.5)	400-1130 (.13-.36)	423	.020	.035

* Indicates experiments used for comparison to the void fraction correlation in previous reports [Chexal and Lellouche (1986), Chexal (1986), Lellouche and Zolotar (1982)].

Table 4-2. Adiabatic steam-water void fraction data

Experiment [ref]	Test Geometry	Hyd Dia mm (ft)	Pressure bar (psia)	Mass Flow kg/s-m2 (Mlb/hr-ft2)	Quality Fraction	Number Data Pts	Mean Error	Standard Deviation
UPFLOW DATA								
Kasai* [1985]	Tube	4.6 (.0151)	70 (1015)	434 (0.32)	0 - .2	35	-.010	.032
Beattie-Sugawara [1986]	Tube	73.9 (.225)	2, 10, 70 (29, 145, 1015)	41 - 678 (.03 - .50)	.03 - .56	54	-.064	.051
Carrier* [1963]	Tube, steam bubbling thru water	456 (1.5)	41 - 136 (600 - 2000)	1.4 - 13.6 (.001 - .010)	1.0	60	-.031	.072
Hughes [1958]	Tube	168 (.522)	83 - 166 (1200 - 2400)	27 - 293 (.02 - .29)	.05 - .22	55	-.010	.027
Turnage-Davis [1979]	Tube	89 (.292)	7.25 (105)	20-300 (.015-.22)	.004-0.48	17	-.034	.086
Hall-Ardron* [1978]	Tube, steam bubbling thru water	105 (.345)	1-4 (14.5 - 58)	.01 - .66 (.00001 - .00049)	1.0	19	.016	.037
Takeuchi [1992]	Tube	175 (.573)	6.9 (1000)	22 - 192 (.016 - .14)	.06 - .40	7	-.069	.016
HORIZONTAL FLOW DATA								
Pye [1984]	Tube	22 (.072)	40 - 180 (580 - 2610)	271 - 1050 (.02 - .43)	.04 - .97	60	-.016	.091
Rajan-Daymond [1979]	Tube	50, 75 (.164, .2461)	54.8 (780)	176 - 2550 (.13 - 1.88)	.01 - .76	77	-.006	.074
COCURRENT DOWNFLOW DATA								
Petrick* [1962]	Tube	49.3 (.162)	41, 69, 103 (600, 1000, 1500)	163 - 1256 (.12 - .83)	0 - .11	144	.024	.048

* Indicates experiments used for comparison to the void fraction correlation in previous reports [Chexal and Lellouche (1986), Chexal (1986), Lellouche and Zolotar (1982)].

Low pressure-low flow data

These conditions are typical of a large break LOCA and are expected to occur during core uncovery and reflood conditions. The core void fraction has a strong effect on heat transients and discharge flows during blowdown and reflood.

Hall-Ardron (1978) - These tests were conducted with a nineteen rod bundle. Void measurements were made in the bundle and above the bundle.

Wong-Hochreiter (1981) - This data was taken in a 161-rod assembly typical of a 17x17 PWR fuel bundle design.

Jowitt (1982) - This is 61 rod boiloff data

Large diameter data

This data provides void fraction behavior at large diameters. This geometry is also important for correlation qualification.

Beattie-Sugawara (1986) - This data was taken in a vertical test section, 0.07 m in diameter at a pressure of 7 MPa and over a range of mass fluxes.

Carrier (1963) - This low-flow data was taken for steam bubbling through water in a 0.45 m diameter pipe over a range of pressures.

Hughes (1985) - This data in a 0.17 m diameter tube covered a wide range of pressures and flows.

Takeuchi, Young and Hochreiter (1992) - This data was taken in a 0.175 m tube, at a pressure of 6.9 kPa and over a range of flows typical of a PWR steam generator riser.

Predictions of all of the vertical upflow steam-water data are shown in Fig. 4-1. More detail about the individual experiments is presented by Chexal (1991). The mean error and standard deviation for the correlation's prediction of each data set are shown in Tables 4-1 and 4-2. The definitions of these terms are discussed later.

Horizontal flow data

Horizontal flow data from adiabatic steam water experiments over a wide range of pressures and flows have been compared to the void correlation. These comparisons are shown in Fig. 4-2. The mean error and standard deviation for each data set is also shown in Table 4-2.

Pye (1984) - This data taken in a 22 mm diameter tube covers a wide range of pressurized flows.

Rajan-Daymond (1979) - This data taken in 50 mm and 74 mm tubes were all taken at 5.48 MPa and covered a range of mass flows.

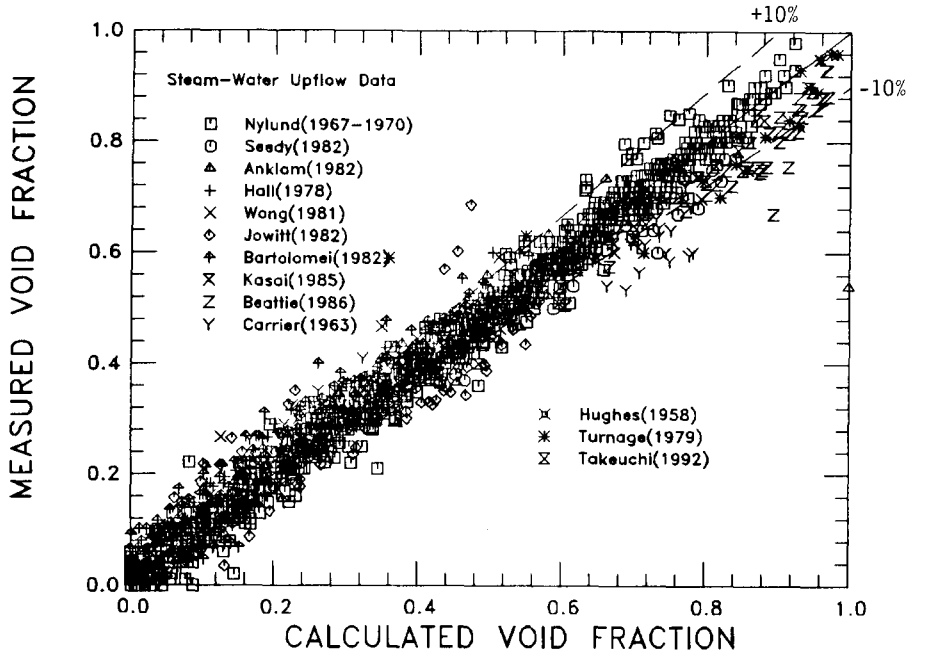

Fig. 4-1. Steam-Water Upflow Data

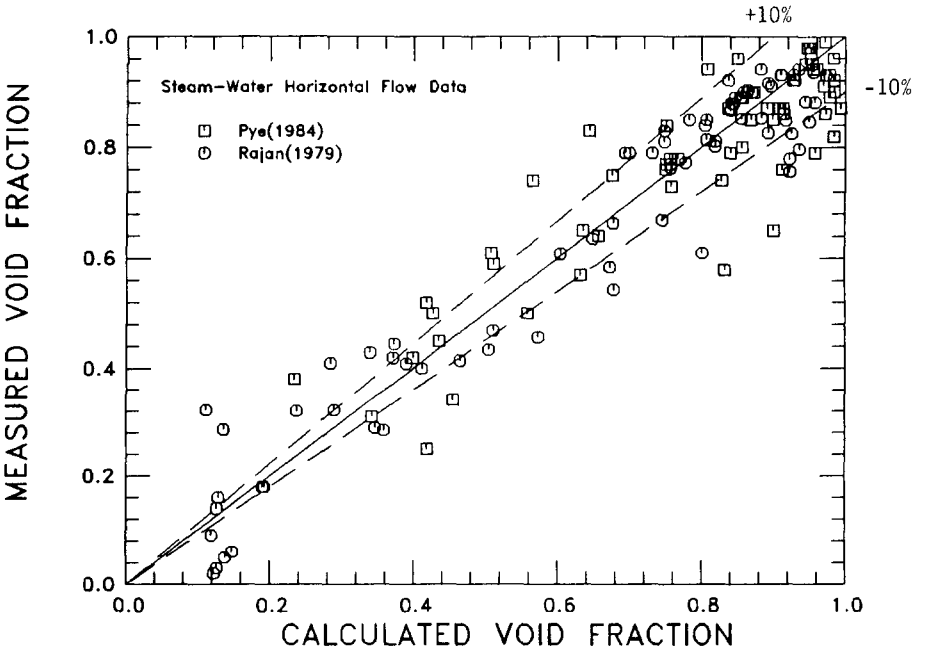

Fig. 4-2. Steam-Water Horizontal Flow Data

Steam-water vertical downflow data

Predictions of adiabatic steam-water downflow data from one experiment are shown in Fig. 4-3. The mean error and standard deviations are also shown in Table 4-1.

Petrick (1962) - This adiabatic void data was taken in a 49 mm tube covers a wide range of pressures and flows.

Steam-water countercurrent flow limit data

Predictions of data from two experiments where the steam-water countercurrent flow limit was measured have been included in the correlation data base. Conditions for each test are summarized in Table 4-3. Predictions of this data are shown in Figs. 4-4 and 4-5.

Jones (1971) - These tests measured the CCFL characteristics of a BWR inlet orifice. Data for three orifice sizes were obtained at low pressure.

Thomas-Combs (1983) - This data, at pressures up to 0.7 MPa measured the CCFL characteristics of a PWR fuel bundle upper-tie plate.

5.0 COMPARISON WITH AIR-WATER DATA

The Chexal-Lellouche fluid parameter, L, which appears in the equation for the distribution parameter, C_0, is modified for application to various fluid types. To correlate air-water data, L was made a function of void fraction only. As noted earlier, the pressure range in the available air-water data was not large and a pressure dependence could not be observed. The data base of cocurrent air-water flow used for comparison to the correlation is listed in Table 5-1 and the countercurrent flow limit data is listed in Table 5-2.

Vertical upflow data

Vertical upflow air-water data compared to the correlation are taken from nine different experiments, with diameters ranging from 0.01 to 0.3 m and mass flow from near zero to 5500 kg/s-m^2. All of the vertical upflow air-water data are shown in Fig. 5-1. Comparisons of predictions with the data from the individual experiments and detailed descriptions of the experiments are presented by Chexal (1991). The mean error and standard deviation for each data set is shown in Table 5-1.

Horizontal flow data

Horizontal flow air-water data from five different experiments have been compared to the correlation. Comparisons to this data are shown in Fig. 5-2. The horizontal air water data also covers a wide range of diameter and mass flows. One data set by Fukano (1987) tested air-water horizontal and near-horizontal flows. All of this data was taken at relatively high void fraction, greater than 0.8. The near-horizontal data have also been included in the data shown in Fig. 5.2. Comparisons of predictions with the data from the individual experiments are presented by Chexal (1991). The mean error and standard deviation for each data set is shown in Table 5-1.

Vertical downflow data

Predictions of air-water downflow data are shown in Fig. 5-3. The vertical downflow data are from three different experiments. The ranges of diameter and mass flow for the downflow data are shown in Table 5-1. Comparisons of predictions with the data from the individual experiments are presented in (4). The mean error and standard deviation for each data set is shown in Table 5-1.

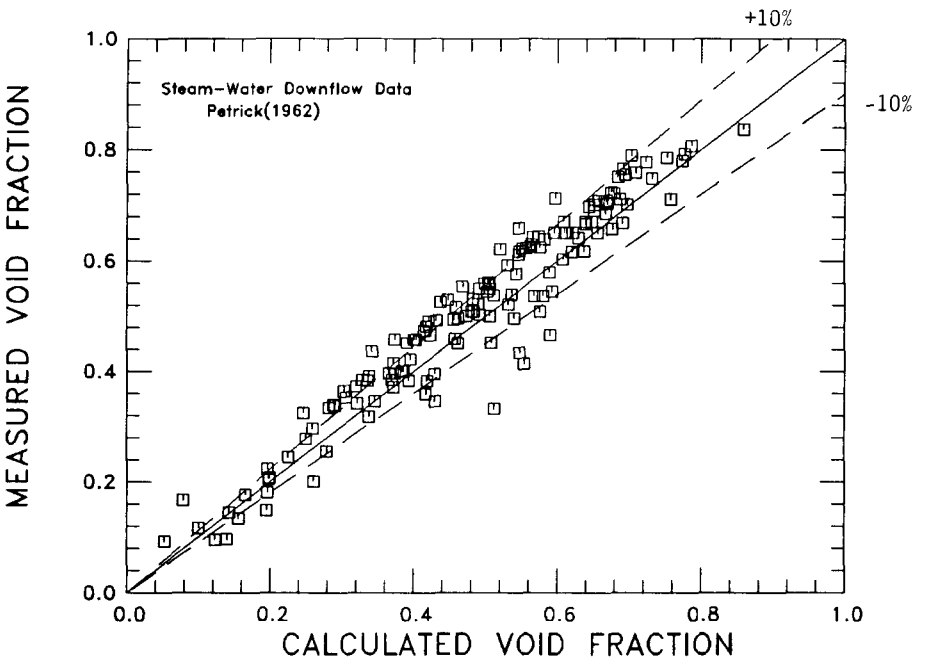

Fig. 4-3. Steam-Water Downflow Data

Table 4-3. Steam-water countercurrent flow limit data

Experiment [ref]	Geometry	Hyd dia mm (ft)	Pressure bar (psia)	Vapor Superficial Velocity m/s (ft/s)	Liquid Superficial Velocity m/s (ft/s)
Jones* [1977]	Vertical Orifice	61.8, 37.6, 31.9 (.203, .123, .105)	1.03 (15)	6 to 24 (20 to 80)	.003 to -.19 (-.01 to -.63)
Thomas-Combs* [1983]	Bundle Upper Tie Plate	10.5 (.034)	6.9, 4.5, 2.1 (100, 65, 35)	5 to 18 (15 to 60)	-.003 to -.14 (-.01 to -.47)

* Indicates experiments used for comparison to the void fraction correlation in previous reports [Chexal and Lellouche (1986), Chexal (1986), Lellouche and Zolotar (1982)].

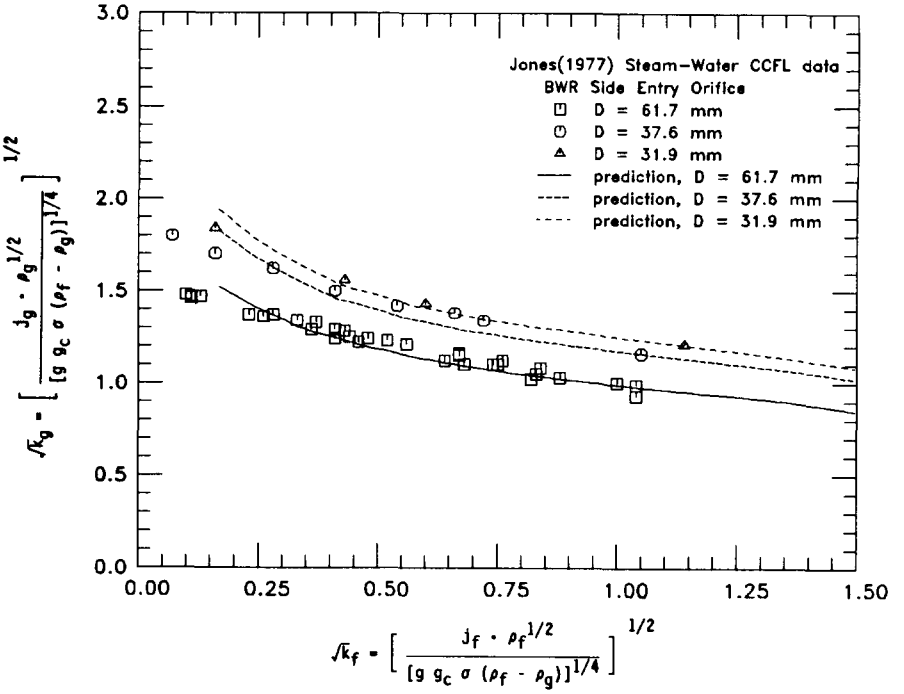

Fig. 4-4. Steam-Water CCFL Data, BWR Fuel Bundle Orifice

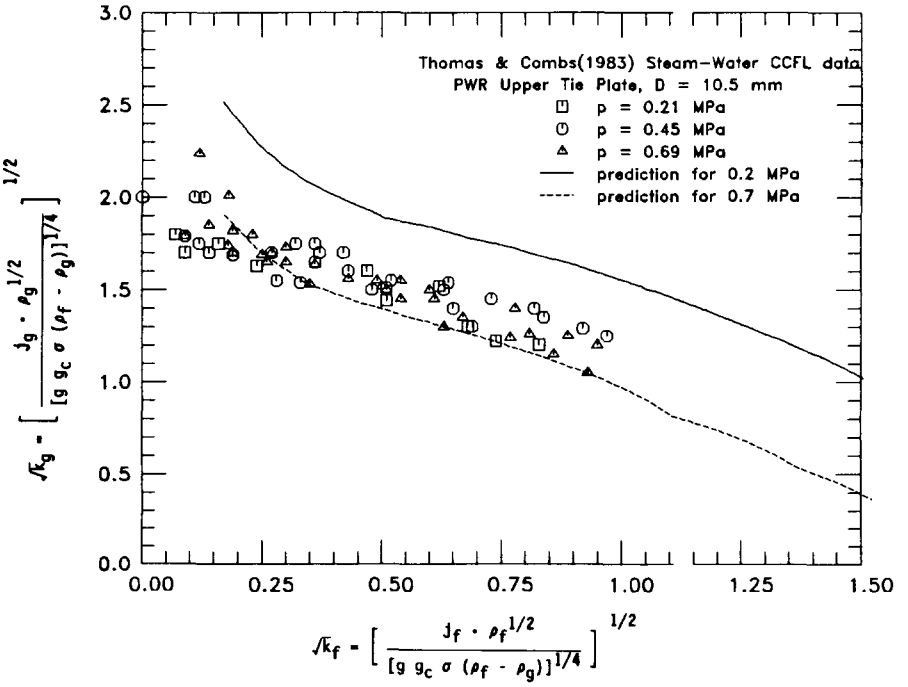

Fig. 4-5. Steam-Water CCFL Data, PWR Upper Tie-Plate

Table 5-1. Air-water void fraction data

Experiment [ref]	Test Geometry	Hyd dia mm (ft)	Pressure bar (psia)	Temp C (°F)	Mass Flow kg/s-m2 (Mlb/hr-ft2)	Air Mass Fraction	Number Data Pts	Mean Error	Standard Deviation
UPFLOW DATA									
Hall-Ardon [1978]	Pipe, air bubbling through water	.105 (.345)	1-4 (14.5-58)	20 (68)	0.18-2.30 (.0001-.0017)	1.0	34	-.039	.047
Smissaert [1963]	Pipe	70 (0.229)	1.01 (14.7)	21 (70)	0.3-310 (.0002-.23)	.001-1.0	161	.007	.052
Tapucu [1980]	Rectangular Channel	12.7 (.0415)	1.19-2.33 (17.3-33.8)	20 (68)	1030-3660 (0.76-2.70)	.00006-.008	99	.012	.024
Hashemi [1986]	Pipe	102, 305 (0.334, 1.0)	1.03-1.17 (14.9-16.9)	20 (68)	.04-490 (0-0.36)	.00003-1.0	31	.027	.080
Schleappi [1988]	Pipe	50.8 (0.167)	2.48-3.93 (36-57)	16-37 (60-99)	460-2800 (.34-2.06)	.001-.025	32	-.071	.030
Borishansky [1977]	Pipe	11 (0.036)	1.14 (16.5)	21 (70)	490-2900 (.36-2.14)	.00004-.019	46	-.012	.041
Turnage [1979]	Pipe	89 (0.292)	1.03 (14.7)	21 (70)	150-4060 (0.11-2.99)	.00004-.316	16	-.063	.046
deMello [1975]	Pipe	36 (0.118)	1.11 (16.1)	23 (73.4)	110-560 (0.08-0.41)	.0001-.0013	23	.049	.032
HORIZONTAL FLOW DATA									
Fukano* [1987]	Pipe	26 (0.125)	1.03-1.38 (15-20)	20 (68)	54-460 (.04-.34)	.035-.356	79	-.018	.039
Simpson [1981]	Pipe	127 (0.417)	1.24-1.38 (18-20)	11-23 (52-73)	3600-4700 (2.63-3.46)	.001-.006	13	-.008	.020
Tapucu [1980]	Rectangular Channel	12.7 (.0415)	1.08-1.91 (15.7-27.7)	20 (68)	760-4180 (0.56-3.08)	.0001-.011	62	.013	.037
Kowalski [1986]	7-Rod Bundle	10 (.03409)	2.25 (32-63)	20 (68)	54-3200 (.04-2.36)	.0002-.447	80	.026	.061
DOWNFLOW DATA									
Oshinowo [1974]	Pipe	25 (.0819)	1.72 (25)	18 (65.0)	150-2000 (0.11-1.46)	.0005-.279	70	-.048	.038
Sokolov [1969]	Pipe	50 (.164)	1.01 (14.7)	27 (80)	780-2000 (.59-1.47)	.00007-.001	34	.006	.061
DATA AT DIFFERENT ANGLES									
Beggs [1972]	Pipe	25.4, 38.1 (.083, .125)	2.56-6.81 (37.2-98.8)	3-36 (38-96)	60-5500 (.04-4.09)	.0008-.833	621	.003	.038

* Horizontal flow and inclined at 10 from horizontal

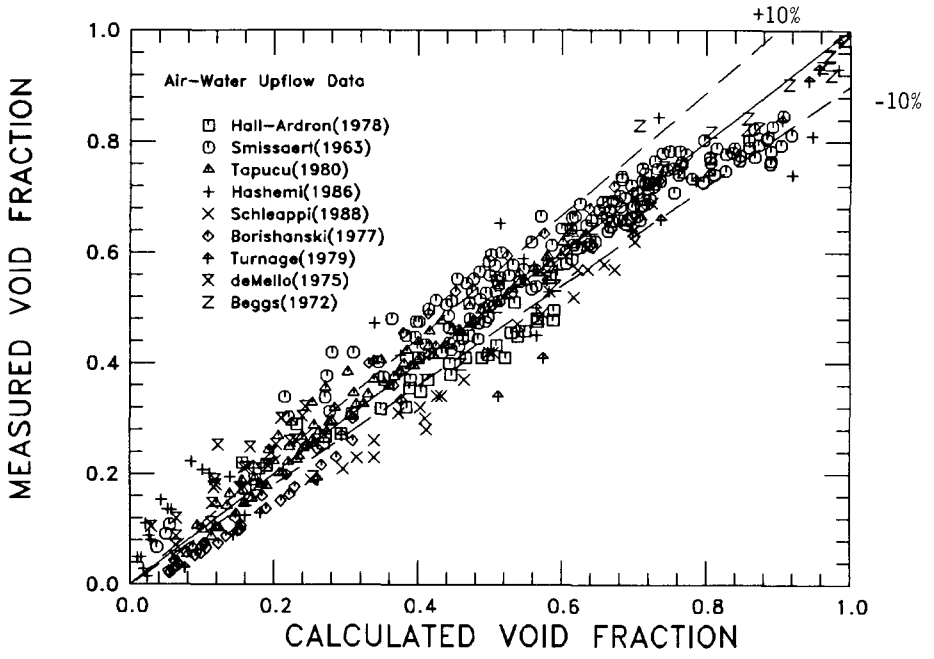

Fig. 5-1. Air-Water Upflow Data

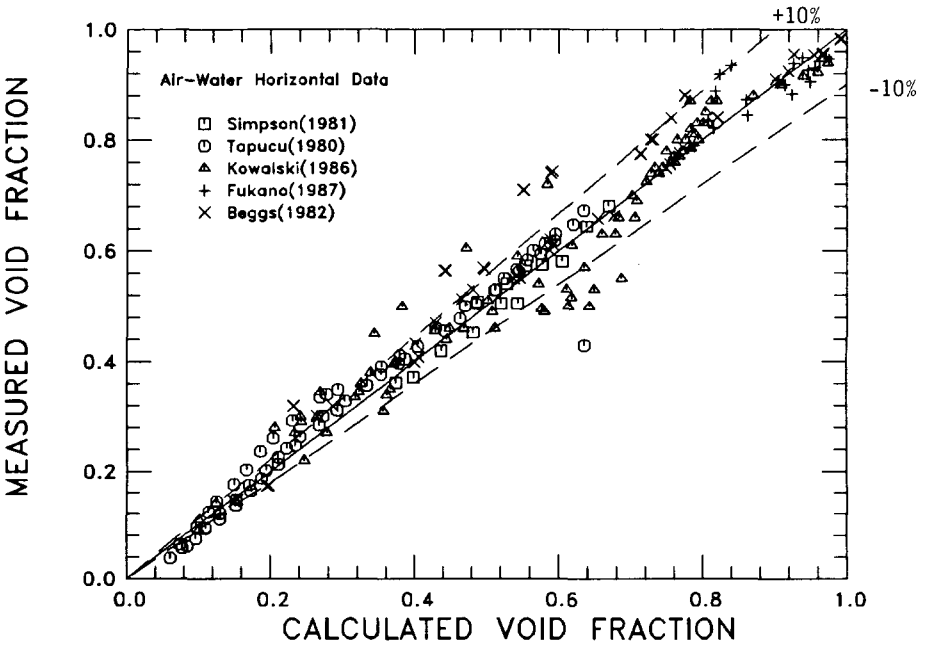

Fig. 5-2. Air-Water Horizontal Flow Data

Table 5-2. Air-water countercurrent flow limit data

Experiment [ref]	Geometry	Hyd dia mm (ft)	Pressure bar (psia)	Vapor Superficial Velocity m/s (ft/s)	Liquid Superficial Velocity m/s (ft/s)
Thomas-Combs [1983]	Bundle Upper Tie Plate	10.5 (.034)	1.10 (16.0)	3.0 to 5.6 (10.0 to 18.3)	.01 to .09 (0.4 to 0.30)
Bharathan [1979]	Tube	25, 51 (.08, .17)	1.01 (14.7)	2.00 to 8.25 (6.6 to 27.1)	~0 to 0.18 (~0 to 0.6)

Inclined flow data

An air-water experiment which provided important benchmarking data for the correlation was by Beggs (1972). In these tests, void fraction was measured in two different diameter pipes, inclined at angles varying from vertical upflow to vertical downflow. Data from these tests were used to demonstrate the applicability of the method used by the correlation to predict flow in a pipe at an angle. Comparisons of predictions with this data are shown in Fig. 5-4. A more detailed description of the experiment and comparisons to the individual data sets is presented by Chexal (1991). The mean error and standard deviation for this data is shown in Table 5-1.

Countercurrent flow limit data

Predictions of data from two experiments where the air-water countercurrent flow limit was measured are shown in Figs. 5-5 and 5-6. The experiment which measured countercurrent steam-water flow limit in a PWR upper tie plate also included air-water measurements (Thomas and Combs, 1983). In addition, air-water countercurrent flow limit data taken in a tube have been included (Bharathan, 1978), Each of these experiments are discussed in more detail in Chexal (1991).

6.0 CONCLUSIONS

The Chexal-Lellouche void fraction correlation was developed originally to provide a continuous void fraction model for use in the light water reactor industry. The correlation was qualified over a wide range of thermodynamic conditions which correspond in the reactor to both normal operating conditions and accident conditions. In this paper and the companion report by Chexal (1991), the correlation has been expanded to include an even wider range of applications.

Steam water applications

The qualification data base for the Chexal-Lellouche void fraction correlation has been extended to cover horizontal steam-water flows and the correlation has been generalized for flow at any orientation, based on comparisons to air-water data. For horizontal flow, the drift velocity used by the correlation does not go to zero but retains a positive value.

To facilitate the use of the void fraction correlation for steam-water applications, the FORTRAN source for a subroutine which implements the correlation is available from EPRI, through the senior author of this paper, for those interested in using the correlation in their own computer program.

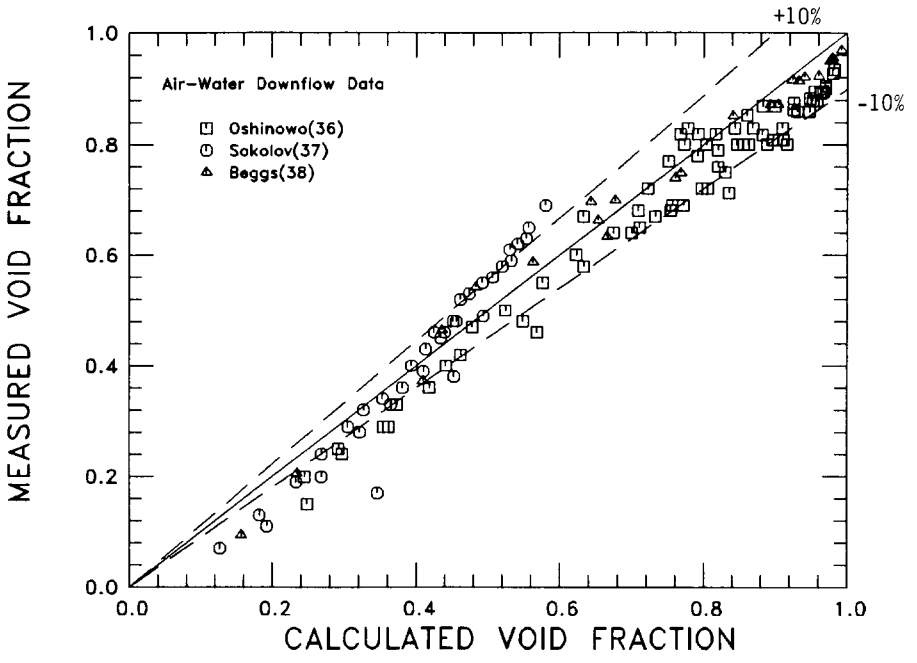

Fig. 5-3. Air-Water Downflow Data

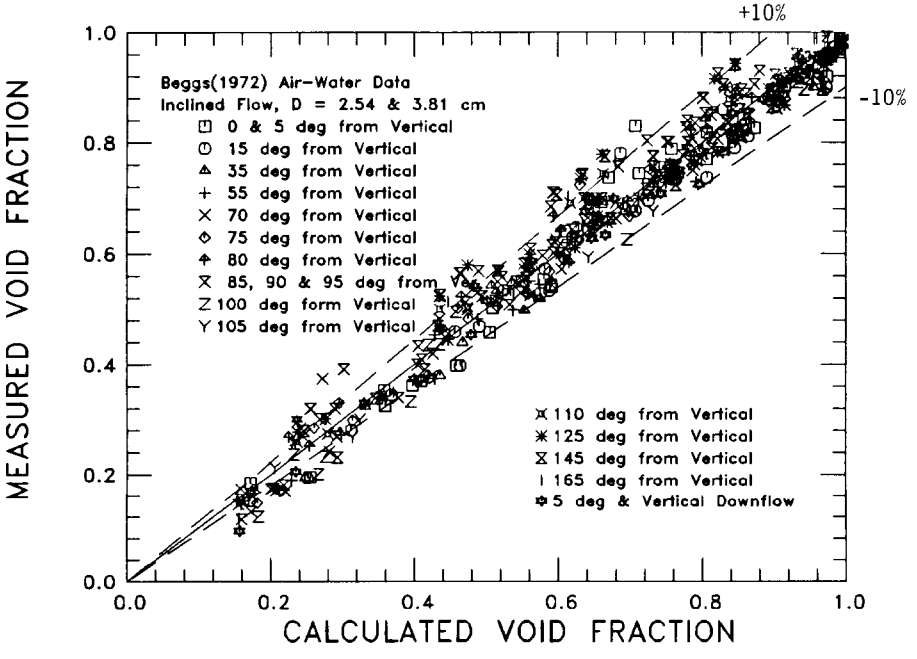

Fig. 5-4. Air-Water Data at Various Inclinations

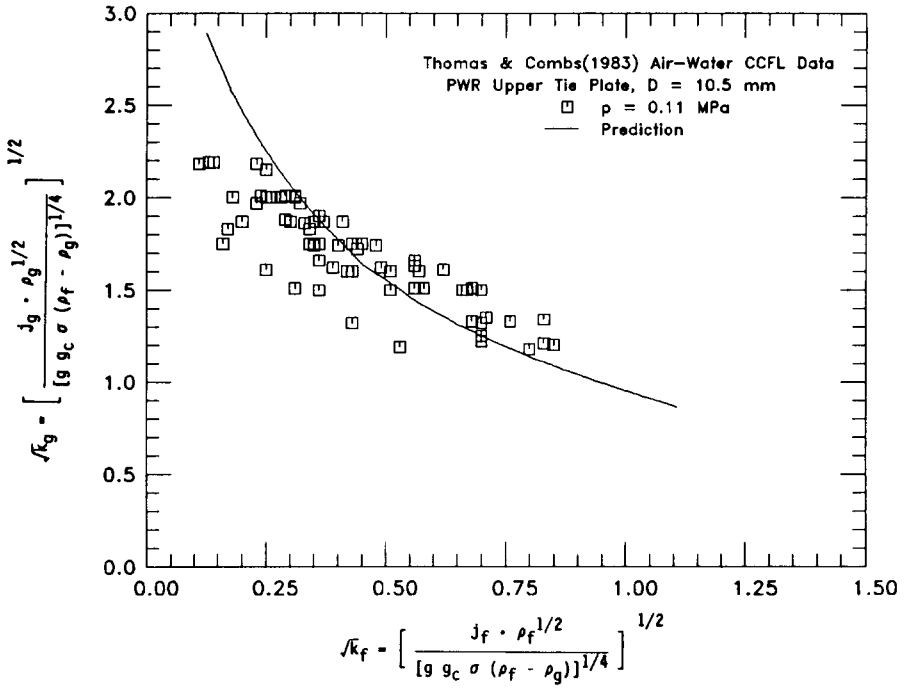

Fig. 5-5. Air-Water CCFL Data, PWR Upper Tie-Plate

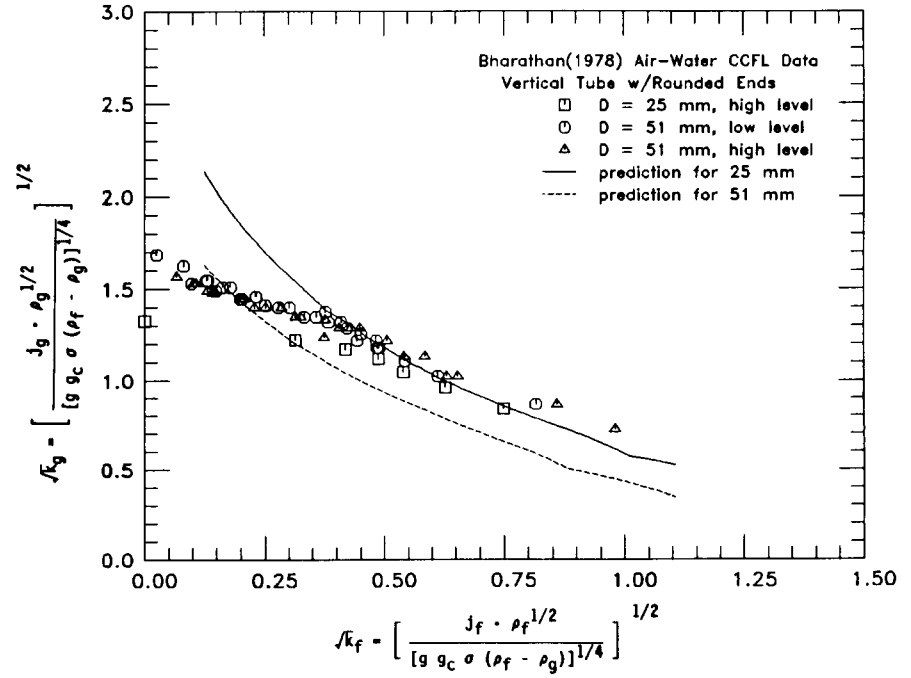

Fig. 5-6. Air-Water CCFL Data, Vertical Tube Data

Air-water applications

The application of the void fraction correlation to air-water has also been demonstrated. The air-water predictions were made by the Chexal-Lellouche fluid parameter, L, in the distribution parameter part of the correlation, the expression for drift velocity remains unchanged. The air-water data base includes a wide range of conditions, including flow at different orientations. An important conclusion from these comparisons was that for cocurrent downflow, if the flow inclination angle is greater than 10 degrees from horizontal, the void fraction data behaves like vertical downflow. This experimental observation has been incorporated in the correlation parameters for both steam-water and air-water applications.

Other fluids

To demonstrate the application of the void fraction correlation to other fluids, comparisons have been made to void fraction measurements taken in several different refrigerants. These comparisons are discussed in detail by Chexal et al. (1991). In these comparisons the refrigerant properties were used and the distribution parameter correlation was modified, similar to what was done for prediction of the air-water data. While the comparisons were not as good as those obtained for steam-water flows, reasonable agreement with the data was obtained. The success of the correlation in predicting the refrigerant data suggests that with proper selection of the Chexal-Lellouche fluid parameter, as was done in this study, the correlation could be applied to a wide variety of fluids.

REFERENCES

Anklam, T. M and Miller, R. F., "Void Fraction Under High Pressure, Low Flow Conditions in Rod Bundle Geometry," Nuclear Engineering and Design, Vol 75, pp 99-108, 1982.

Bankoff, S. G., "A Variable Density Single-Fluid Model for Two-Phase Flow," Trans. ASME, Series C, 82, 1960, pg. 265.

Bartolomei, G. G., et al., "An Experimental Investigation of True Volumetric Vapour Content with Subcooled Boiling in Tubes," Thermal Engineering, 1982 (3) pp 132-135.

Beattie, D. R. H. and Sugawara, S., "Steam Water Void Fraction for Vertical Upflow in a 73.9 mm Pipe," Int. J. Multiphase Flow, Vol. 12, No. 4, 1986, pp. 641-653.

Beggs, H. D., "An Experimental Study of Two-Phase Flow in Inclined Pipes," Ph.D. Thesis, Department of Petroleum Eng., University of Tulsa, 1972.

Behringer, H., "The Flow of Liquid Gas Mixtures in Vertical Tubes," Zeit. Ges. Kalte-Int., 43, 1936, pp 55-58 (see also AEC TR 1777).

Bharathan, D., Air-Water Countercurrent Annual Flow in Vertical Tubes, EPRI Report NP-780, May 1978.

Borishansky, V. M., Bykov, G. S., Zalentnev, A. F., Forin, B. S., Volukhova, T. G. and Andreyevskiy, A. A., "Void Fraction and Pressure Drop in Two-Phase Upflow at Atmospheric Pressure," Fluid Mechanics, Soviet Research, Vol. 6, Nov-Dec, 1977.

Carrier, F., et al., Steam Separation Technology Under the Euratom Program, Allis-Chalmers Atomic Energy Division Report No. ANCP-63021, July 1963.

Chexal, B. and Lellouche, G. S., A Full-Range Drift-Flux Correlation for Vertical Flows, EPRI-NP-3989-SR (Revision 1), September 1986.

Chexal, B., et al., An Assessment of Eight Void Fraction Models for Vertical Flows, EPRI-NSAC-107, December 1986.

Chexal, B., et al., The Chexal-Lellouche Void Fraction Correlation for Generalized Applications, NSAC-139, February 1991.

Chexal, B., Horowitz and Lellouche, G., "An Assessment of Eight Void Fraction Models for Vertical Flows," EPRI Report NSAC-107, Dec. 1985, also published in Nuclear Engineering and Design, 126, 1991, pp. 71-88.

deMello, R. E. F., Behard, M. R. and Martinee, E. W., Study of the Void Fraction in a Two-Phase Air/Water Flow in a Vertical Tube, Instituta de Enegia Atamica, Report No. 378, January 1975.

Fukano, T. and Ousaka, A., Hold-up, Frictional Pressure Drop and Circumferential Film Thickness Distribution of Air-Water Two-Phase Annular Flow in Horizontal and Near Horizontal Flow, Proceedings of the 1987 ASME-JSME Thermal Engineering Joint Conference.

Griffith, P. and Wallis, G. B., Two-Phase Slug Flow, Trans Asme, Series C, Aug. 1961, p. 307.

Hall, P. C. and Ardron, K. H., "Prediction of Void Fraction in Low Velocity Vertical Bubbling Flows," paper presented at the European Two Phase Flow Group Meeting, Stockholm, Sweden, 1978.

Hashemi, A., Two-Phase Flow Regimes and Carry-Over in a Large Diameter Model of a PWR Hot Leg, EPRI Report NP-4530, April 1986.

Hughes, T., Steam-Water Mixture Density Studies in a Natural Circulation High Pressure System, Babcock and Wilcox, G. Report No. 5435, 1958.

Ishii, M., Thermo-Fluid Dynamic Theory of Two-Phase Flow, Chapters IX and X, Eyrolles, Paris, 1975.

Jones, D., Test Report TLTA Components CCFL Tests, NEDG-NUREG-23732, 1977.

Jowitt, D., A New Voidage Correlation for Level Swell Conditions, AEEW-R-1480, UKAEA Winfrith, 1982.

Kasai, S., et al., Void Fraction Measurements Under Simulated BWR Thermal-Hydraulic Conditions, presented at Proceedings of Third International Topical Meeting on Reactor Thermal Hydraulics, Newport, Rhode Island, October 1985.

Kowalski, J. E., Krishnan, V. S. and McCallam, C. K., Two-Phase Air-Water and Freon Gas-Water Studies in Horizontal Channels, CANDEU-85-13, AECL Whiteshell National Research Establishment, Pinawa, Manitoba, 1986.

Lellouche, G. S. and Zolotar, B. A., Mechanistic Model for Predicting Two-Phase Void Fraction for Water in Vertical Tubes, Channels, and Rod Bundles, EPRI-NP-2246-SR, Special Report, February 1982.

Lellouche, G. S., "An Analytical Solution for the Subcooled Flow Quality," ANS Transactions, Vol 57, pp 345, 346, 1988.

McFadden, et al., "RETRAN-03 A Program for Transient Thermal-Hydraulic Analysis of Complex Fluid-Flow Systems," EPRI Report NP-7450-CCML, Vol. 1, July 1991.

Neal, L. G., "An Analysis of Slip in Gas-Liquid Flow Applicable to the Bubble and Slug Flow Regimes," Report KR-62, Kjeller Research Establishment, Kjeller, Norway, Dec. 1963.

Nicklin, D. J., Wilkes, J. O. and Davidson, J. F., "Two Phase Flow in Vertical Tubes," Trans. Inst. of Chem. Engrs., 40, 1962, p. 61

Nylund, O., et al., Hydrodynamic and Heat Transfer Measurements on a Full-Scale Simulated 36-Rod BHWR Fuel Element with Non-Uniform Axial and Radial Heat Flux Distribution, FRIGG-4, 1970.

Nylund, O., et al., Hydrodynamic and Heat Transfer Measurements on a Full-Scale Simulated 36-Rod Marviken Fuel Element with Uniform Heat Flux Distribution, FRIGG Loop Project, FRIGG-2, 1968.

Nylund, O., et al., Hydrodynamic and Heat Transfer Measurements on a Full-Scale Simulated 36-Rod Marviken Fuel Element with Non-uniform Radial Heat Flux Distribution, FRIGG-3, 1969.

Nylund, O., et al., Measurements of Hydrodynamic Characteristics, Instability Thresholds, and Burnout Limits for 6-Rod Clusters in Natural and Forced Circulation, FRIGG Loop Project, FRIGG-1, 1967.

Oshinowo, T., Charles, M. E., "Vertical Two-Phase Flow: Part II. Holdup and Pressure Drop," Canadian J. Chem. Eng., Vol. 52, August, 1974.

Personal Communication, Crag Peterson, Computer Simulation and Analysis Inc., July 1991.

Personal Communication, Mike Cappiello, Los Alamos National Laboratory, August 1991.

Petrick, M., A Study of Vapour Carryunder and Associated Problems, ANL-6581, July 1962.

Pye, J. W., Determination of Steam-Water Voids in a Horizontal Tube Using a Flash X-ray Technique, CEGB Report TPRD/M/1441/N84, November 1984.

Rajan, V. S. V. and Daymond, D. C. S., A Study of Steam-Water Flow in Horizontal Pipes, WNRE-225-31, AECL Whiteshell Nuclear Research Establishment, Pinawa, Manitoba, 1979.

Schleappi, D. D. and Moskal, T. E., Air-Water Two-Phase Characteristics of MIST Turbine Meters, Babcock and Wilcox, RDD:88:6022-01-01:01, March 4, 1988.

Seedy, D. and Muralidhoran, BWR Low-Flow Bundle Uncovery Test and Analysis, EPRI-NP-1781, June 1982.

Simpson, H. C., Rooney, D. H., Grattan, E., Alsamarrae, F. A. A., Two-Phase Studies in Large Diameter Horizontal Tubes, National Engineering Lab., Ensk Kilbride, University of Stratchclyde, Glasgow, December 1981.

Smissaert, G. E., Two Component Two-Phase Flow Parameters for Low Circulation Rates, ANL-6755, July 1963.

Sokolov, V. N., Davydov, I. V., Domanskii, I. V., "Gas Content in Tubular Bubbling Reactors of the Displacement Type," J. App. Ch. USSR, Vol. XLII, Part 4, 1969.

Street, J. R., and Tek, M. R., Dynamics of Bullet Shaped Bubbles Encountered in Gas Liquid Slug Flow, Abstract No. IDE, 56 Annual AIChE meeting, Dec., 1-5, 1963.

Takeuchi, K., Young, M. and Hochreiter, L., "Generalized Drift Flux Correlation for Vertical Flow, Nuclear Science and Engineering, Vol 112, 170-180, 1992.

Tapucu, A. and Gencay, S., Experimental Investigation of Mass Exchanges Between Two Laterally Interconnected Two-Phase Flow, Part 1: Experimental Results on Vertical Flow, IGN-354, Ecole Polytechnique de Montreal, University of Montreal, Quebec, 1980.

Tapucu, A. and Gencay, S., Experimental Investigation of Mass Exchanges Between Two Laterally Interconnected Two-Phase Flow, Part 2: Experimental Results on Horizontal Flow, IGN-394, Ecole Polytechnique de Montreal, University of Montreal, Quebec, 1980.

Thomas, D. and Combs, S., Measurement of Two-Phase Flow at the Core/Upper Plenum Interface for a PWR Geometry Under Simulated Reflood Conditions, NUREG/CR-3138, 1983.

Turnage, K. G. and Davis, C. E., Two-Phase Flow Measurements with Advanced Instrumented Spool Pieces and Local Conductivity Probes, Union Carbide Corporation Nuclear Division, July 1979.

Wong, S. and Hochreiter, L., Analysis of the FLECHT SEASET Unblocked Bundle Steam-Cooling and Boiloff Tests, EPRI-NP-1460, 1981.

Zuber, N. and Findlay, J., "Average Volumetric Concentration in Two-Phase Flow Systems," J. Heat Transfer 87, 453, 1965.

Zuber, N., et al., Steady State and Transient Void Fraction in Two-Phase Flow Systems, General Electric Co. Report GEAP-5417, Vol. 1, 1967.

APPENDIX A: DRIFT FLUX MODEL BACKGROUND

A.1 HISTORICAL PERSPECTIVE

The drift flux formulation for void fraction provides a means for accounting for the effects of the local relative velocity between the phases as well as the effects of non-uniform flow and concentration distributions.

The first efforts to consider relative velocity effects are attributed to Behringer (1936) who expressed the velocity of a bubble in a bubbly mixture as

$$V_g = \frac{Q_f}{A} + \frac{Q_g}{A} + V_T \tag{A-1}$$

where Q_f and Q_g are the volumetric liquid and vapor flows, A the flow area and V_T the bubble rise velocity in an infinite medium.

The first to consider the effects of non-uniform flow and concentration was Bankoff (1960). He developed an expression for the ratio of the velocities of the phases (the slip ratio) for bubbly flow as

$$S = \frac{V_g}{V_f} = \frac{1-\alpha}{K-\alpha} \tag{A-2}$$

In this expression, V_g and V_f are the average velocities of the vapor and liquid phases, α the average volumetric vapor concentration (void fraction) and K is a flow parameter determined by the velocity and concentration profiles and also a function of pressure, quality and mass flow rate.

Others (Nicklin, et al., 1962 and Neal, 1963) modified Behringer's equation to account for concentration effects by rewriting it as

$$V_g = C_o \left(\frac{Q_f}{A} + \frac{Q_g}{A} \right) + V_T \tag{A-3}$$

Where C_o is a distribution parameter and the expression for bubble rise velocity was taken as

$$V_T = 0.35 \left[g(\rho_f - \rho_g)\, D/\rho_f \right]^{\frac{1}{2}} \tag{A-4}$$

where g is the acceleration of gravity, ρ_g and ρ_f the vapor and liquid densities and D the channel diameter. This bubble rise velocity had been derived earlier by Griffith and Wallis (1961) for slug flow. A similar development by Street and Tek (1963) expressed the vapor velocity as

$$V_g = C_o \left(\frac{Q_f + Q_g}{A} \right) + C_1 \sqrt{gD} \tag{A-5}$$

where C_0 and C_1 were dependent on flow and density distributions.

The method of accounting for the effects of nonuniform velocity and density distributions as well as the effects of local relative velocities between phases was formalized by Zuber and Findlay (1965). Their development for the local vapor velocity and void fraction in terms of the volumetric distribution is the basis of the drift flux formulation. The following development is a somewhat simplified from theirs.

Since the channel average void fraction is of interest, it is convenient to define the average value of a scalar or vector quantity, F, over the channel.

$$\langle F \rangle = \frac{1}{\bar{A}} \int_A F dA \tag{A-6a}$$

Cross-sectional area averaging is useful since parameters that vary in three dimensions can be reduced to quasi-one-dimensional forms. However, information about changes in the direction normal to the main flow is lost by area averaging and must be replaced by empirical information or by using simplified models.

It follows then that the average void fraction over the channel will be given by

$$\langle \alpha \rangle = \frac{1}{\bar{A}} \int_A \alpha dA \tag{A-6b}$$

For constant phase density, the vapor volumetric flow rate through the channel can be expressed in terms of the local vapor velocity and void fraction

$$Q_g = \int_A (V_g \alpha)\, dA \tag{A-7}$$

The channel flow can also be expressed in terms of the channel average void fraction, a weighted mean vapor velocity and the channel area

$$Q_g = A \langle \alpha \rangle \bar{V}_g$$

Solving for the vapor velocity gives

$$\bar{V}_g = \frac{Q_g}{\langle \alpha \rangle \bar{A}} = \frac{1}{\langle \alpha \rangle \bar{A}} \int_A (V_g \alpha)\, dA \tag{A-8}$$

In Eq. A-8, if the vapor volumetric flow rate is known, specifying the weighted mean vapor velocity determines the channel average void fraction. Zuber and Findlay (1965), in their development, expressed the local three-dimensional phase velocities in terms of local volumetric fluxes

j_g = volumetric vapor flux = αV_g

j_f = volumetric liquid flux = $(1-\alpha)V_f$

and the mixture volumetric flux is given by

$$j = j_g + j_f$$

The local vapor velocity is specified in terms of the mixture volumetric flux and a drift velocity, V_{gj}, which is the velocity of the vapor with respect to the mixture. The drift velocity is defined as

$$V_g = j + V_{gj} \tag{A-9}$$

Solving for V_g and substituting this expression into Eq. A-8 for vapor velocity yields

$$\bar{V}_g = \frac{1}{\langle\alpha\rangle A}\int_A (j\alpha)dA + \frac{1}{\langle\alpha\rangle A}\int_A (V_{gj}\,\alpha)dA$$

or

$$\bar{V}_g = \bar{j} + \bar{V}_{gj} \tag{A-10}$$

In this expression, the first term is the weighted mean mixture volumetric flux density, $\bar{j}$, and the second term is the weighted mean drift velocity, $\bar{V}_{gj}$. Finally, consistent with earlier work, a distribution parameter, C_o, is defined as the ratio of the weighted mean mixture volumetric density, $\bar{j}$, to the section average volumetric flux density, $\langle j\rangle$,

$$C_o \equiv \frac{\bar{j}}{\langle j\rangle} = \frac{1}{\langle j\rangle}\left[\frac{1}{\langle\alpha\rangle A}\int_A (j\alpha)dA\right] = \frac{\langle\alpha j\rangle}{\langle\alpha\rangle\langle j\rangle} \tag{A-11}$$

This gives the following expression for the weighted vapor velocity

$$\bar{V}_g = C_o\langle j\rangle + \bar{V}_{gj} \tag{A-12}$$

In this equation, the weighted mean vapor velocity is related to the distribution parameter, C_o, and the weighted mean vapor drift velocity, $\bar{V}_{gj}$. The advantage that this equation offers is that the effects of density and flow distributions have been separated from the effects of local phase velocity differences.

The weighted mean vapor velocity is next expressed in terms of the void fraction as

$$\bar{V}_g = \frac{\langle\alpha V_g\rangle}{\langle\alpha\rangle} = \frac{\langle j_g\rangle}{\langle\alpha\rangle} \tag{A-13}$$

then the general drift flux formulation for void fraction is given by

$$\langle\alpha\rangle = \frac{\langle j_g\rangle}{C_o\langle j\rangle + \bar{V}_{gj}} \tag{A-14}$$

where the concentration parameter, C_o, and the drift velocity, $\bar{V}_{gj}$, are the parameters in the drift flux void model. Note that if $\bar{V}_{gj}$ is equal to zero and C_o is equal to one, drift flux relationships describe homogeneous flow. If $\bar{V}_{gj}$ is equal to zero but C_o is not equal to one, drift flux relationships yield the so-called slip equations. As Zuber and Findlay (1965) show, C_o is smaller than one when the void concentration is near the wall of the channel, and C_o is larger than one for the reverse condition. Thus for a channel which experiences the entire range of boiling regimes, C_o should vary as first smaller than one, then larger than one and finally going to one. In the early stages of subcooled boiling, the voids exist primarily near the wall, whereas in fully developed boiling the preponderance of voids are in the center of the channel. In the limit when $\langle\alpha\rangle$ goes to one, C_o approaches one and $\bar{V}_{gj}$ approaches zero.

A.2 DRIFT FLUX RELATIONSHIPS

The relationships for the mean vapor velocity, $\bar{V}_g$, and mean liquid velocity, $\bar{V}_f$ in terms of drift flux parameters and total mass flux, G_o, can be derived using the following two equations

$$\text{weighted mean vapor velocity: } \bar{V}_g = \frac{\langle j_g \rangle}{\langle \alpha \rangle} = C_o \langle j \rangle + \bar{V}_{gj} \tag{A-15}$$

$$\text{mass conservation: } \quad G_o A = \rho_f \langle j_f \rangle A + \rho_g \langle j_g \rangle A \tag{A-16}$$

where

G_o = W/A = total mass flux

ρ_f, ρ_g = liquid and vapor densities

$\langle j \rangle$ = $\langle j_f \rangle + \langle j_g \rangle$ = two-phase mixture volumetric flux, the sum of the liquid and vapor volumetric fluxes

W = total mass flow rate

From Eq. A-16

$$\langle j_f \rangle = \frac{G_o - \rho_g \langle j_g \rangle}{\rho_f} \tag{A-17}$$

$$\langle j_g \rangle = \frac{G_o - \rho_f \langle j_f \rangle}{\rho_g} \tag{A-18}$$

To calculate $\bar{V}_g$, vapor velocity, the $\langle j_f \rangle$ from Eq. A-17 can be substituted in Eq. A-15 to give

$$\bar{V}_g = \frac{\langle j_g \rangle}{\langle \alpha \rangle} = C_o \langle j_g \rangle + C_o \left[\frac{G_o - \rho_g \langle j_g \rangle}{\rho_f} \right] + \bar{V}_{gj}$$

or

$$\bar{V}_g = \frac{\frac{C_o G_o}{\rho_f} + \bar{V}_{gj}}{1 - \langle \alpha \rangle C_o \left[1 - \frac{\rho_g}{\rho_f} \right]} \tag{A-19}$$

Similarly, substituting $\langle j_g \rangle$ from Eq. A-18 into Eq. A-15 yields:

$$\left[\frac{G_o - \rho_f \langle j_f \rangle}{\rho_g} \right] (1 - \langle \alpha \rangle C_o) = \langle \alpha \rangle C_o \langle j_f \rangle + \langle \alpha \rangle \bar{V}_{gj}$$

therefore

$$\bar{V}_f = \frac{\langle j_f \rangle}{1-\langle\alpha\rangle} = \frac{(1-\langle\alpha\rangle C_o)\left[G_o - \frac{\langle\alpha\rangle \rho_g \bar{V}_{gj}}{1-\langle\alpha\rangle C_o} \right]}{\rho_f (1-\langle\alpha\rangle)\left[1-\langle\alpha\rangle C_o \left(1 - \frac{\rho_g}{\rho_f} \right) \right]} \tag{A-20}$$

The expression for slip velocity, $\bar{V}_g - \bar{V}_f$ can be obtained by taking difference of Eqs. A-19 and A-20 and is given by

$$\bar{V}_g - \bar{V}_f = \frac{\bar{V}_{gj}\left[1 - \langle\alpha\rangle \left(1 - \frac{\rho_g}{\rho_f} \right) \right] - \frac{G_o (1 - C_o)}{\rho_f}}{\left[1 - \langle\alpha\rangle C_o \left(1 - \frac{\rho_g}{\rho_f} \right) \right] (1-\langle\alpha\rangle)} \tag{A-21}$$

The value of void fraction at the interface between the two-phase mixture and vapor, the "level", $\langle\alpha\rangle^*$, can be obtained at steady-state by equating $\bar{V}_f$ to zero in Eq. A-20.

$$\langle\alpha\rangle^* = \frac{G_o}{\rho_g \bar{V}_{gj} + G_o C_o} \tag{A-22}$$

APPENDIX B SUBCOOLED BOILING MODEL

The subcooled boiling model used in the data comparisons shown in this study is a mechanistic model by Lellouche (1988). In this model, the wall heat flux is divided into boiling and forced convection components. Using an energy balance on the thermal boundary layer, an expression for the vapor generation is derived which can be used to define the onset of subcooled boiling. The vapor generation is given by:

$$\Gamma = \frac{4}{D_H\, h_{fg}} \left[\frac{(h_{fc}/2 + h_B)\,(T_w - T_f) - h_c\,(T_f - T_l)}{1 + \rho_l/\rho_g\,(h_f - h_l)/h_{fg}} \right] \tag{B-1}$$

where

D_H = hydraulic diameter

ρ_l, ρ_g = subcooled liquid and saturated vapor density

h_l, h_f, h_{fg} = subcooled liquid, saturated liquid enthalpy and the heat of vaporization

T_w, T_l, T_f = wall, subcooled liquid and saturated liquid temperature

h_c, h_{fc}, h_B = condensation, forced convection and boiling heat transfer coefficients

For a fixed pressure, the vapor generation can be evaluated as a function of distance along the heated channel, z. The onset of subcooled boiling occurs when the vapor generation term goes through zero, $\Gamma(z_D) = 0$.

In the Lellouche model, the following correlations are used for the various heat transfer coefficients.

Forced Convection

The Dittus-Boelter correlation is used with a modified constant to account for rod-bundle geometry.

$$h_{fc} = C_{fc}\, Re_l^{0.8}\, Pr_l^{0.4}\, k_l/D_H \tag{B-2}$$

where

$$C_{fc} = \begin{cases} 0.023 \text{ for heated tubes} \\ 0.013 + 0.033E \text{ for rod bundles} \end{cases}$$

E = fraction of the unblocked flow area available for flow

$Re_l = (1\text{-}X)W\, D_H/\mu_l A$, liquid Reynolds number

W = channel flow

A = channel flow area

$Pr_l = \rho_l C_{pl}/k_l$, liquid Prandtl number

k_l = liquid conductivity

C_{pl} = liquid specific heat

μ_l = liquid viscosity

Condensation

The Hancox-Nicoll correlation is used for the condensation heat transfer coefficient, defined in the following manner:

$$h_c = C_c \, Re_l^{0.662} \, Pr_l \, k_l/D_r \tag{B-3}$$

where

$$C_c = \begin{cases} 0.2 \text{ for heated bundles} \\ 0.1 \text{ for rod bundles} \end{cases}$$

D_r = rod diameter

Boiling

For boiling heat transfer, the Thom correlation is used:

$$h_B = h_B^o \, (T_w - T_f) \tag{B-4a}$$

where

$$h_B^o = 193e^{p/630} \text{ , heat transfer coefficient in Btu/hr-ft}^2\text{-°F} \tag{B-4b}$$

p = pressure in psia

Note that the Thom model is an empirical fit for steam-water flows only. For other fluids, a boiling correlation appropriate for that fluid should be used.

Once the location of the onset of subcooled boiling is determined, the flow quality, X, in the heated channel is determined by numerically integrating the following equation:

$$\frac{dX}{dz} = \frac{S(dX_e/dz) - C \, (X-X_e)/(1-X_e)}{1 + \frac{\rho_f}{\rho_g} (X-X_e)(1-X)} \tag{B-5}$$

where

X_e = channel equilibrium quality

$S = (h_B + h_{fc}/2)(h_B + h_{fc})$

$$C = 4(h_c + Sh_{fc})/(W\ D_H\ Cp_l/A)$$

The void fraction is then calculated using the superficial liquid and vapor velocity based on the flow quality.

When the flow quality is calculated using the above equation, it will approach and, depending on the numerical scheme, even slightly exceed the equilibrium quality. In the present calculations, as soon as the flow quality came within .01% of the equilibrium quality, the flow quality was set equal to the equilibrium quality.

Since the value of S depends on the wall temperature, the model is not directly integrable. Statistically (Lellouche, 1988) we find that if S is evaluated at the detachment point $S=S(Z_D)$ (which must in any case be determined) and then kept at that value, the results are quite satisfactory.